Available online at www.sciencedirect.com
ScienceDirect
International Journal of Heat and Mass Transfer 50 (2007) 3265–3277
International Journal of HEAT and MASS TRANSFER
www.elsevier.com/locate/ijhmt

A three-dimensional inverse problem in estimating the applied heat flux of a titanium drilling – Theoretical and experimental studies

Cheng-Hung Huang [a,*], Li-Chun Jan [a], Rui Li [b], Albert J. Shih [b]

[a] Department of Systems and Naval Mechatronic Engineering, National Cheng Kung University, Tainan 701, Taiwan, ROC
[b] Department of Mechanical Engineering, University of Michigan, Ann Arbor, MI 48109-2125, USA

Received 22 June 2006; received in revised form 26 January 2007
Available online 28 March 2007

Abstract

The applied heat flux on the drilling surface of drilling tool is estimated in the present three-dimensional inverse heat conduction problem. The inverse algorithm utilizing the Steepest Descent Method (SDM) and a general purpose commercial code CFX4.4 is applied successfully in this study based on the simulated and measured temperature distributions with time at four sensors embedded on the drilling surfaces. The numerical experiments are considered at the first stage to illustrate the validity of inverse determination of the unknown heat flux using exact and error measurements. Experimental data are then used to estimate the actual heat flux along the drilling edge at two different drill peripheral cutting speeds. Results of both the numerical and experimental examinations show that the reliable estimated heat flux can be obtained by using the present inverse algorithm.

1. Introduction

Titanium alloys are excellent candidates for high performance applications owing to their high strength to weight ratio and excellent corrosion resistance, maintained even at high temperature. However, the machinability of titanium and its alloys is generally poor owing to several inherent properties of the materials. During machining, titanium alloys have a tendency to weld to the cutting tool, thus leading to chipping and premature tool failure. Its low thermal conductivity increases the temperature at the tool/workpiece interface, which affects the tool life adversely. Additionally, its high strength maintained at elevated temperature and its low modulus of elasticity further impairs its machinability.

Ti drilling has been widely utilized in industry, the research publications in this subject can be found, but not many, in the literature. For instance, a series of experiments in drilling of Ti–6Al–4V have been conducted by Sakurai et al. [1–3]. Arai and Ogawa [4] studied the high pressure (7 MPa) cutting fluid assisted drilling. Cantero et al. [5] focused on the dry drilling tool wear and workpiece subsurface damage.

Drilling temperature and heat flux at the tool–chip interface have long been recognized as major factors that influence the tool performance. During drill machining, high heat fluxes, consequently high temperatures, are imposed on the region of the drilling edges. The rate of wear of the drilling tool and the friction between the workpiece and tool depend strongly on these heat fluxes. However, direct measurement of temperature at the tool–chip interface using traditional type sensors is impossible due to the cutting movement and the presence of the chip. Due to the fact that the direct sensing of the tool–chip interface temperature is difficult, the use of the techniques of inverse heat conduction problems is a good alternative since this technique takes into account temperatures measured from accessible positions.

The 3-D inverse problems for an irregular domain are still limited in the literature. The technique of the 3-D inverse problems of irregular domain in utilizing an

* Corresponding author. Tel.: +886 62747018; fax: +886 62747019.
E-mail address: chhuang@mail.ncku.edu.tw (C.-H. Huang).

0017-9310/$ - see front matter © 2007 Elsevier Ltd. All rights reserved.
doi:10.1016/j.ijheatmasstransfer.2007.01.031

Nomenclature

C_p	heat capacity
h	heat transfer coefficient
$J[q(t)]$	functional defined by Eq. (2)
$J'(S_d,t)$	gradient of functional defined by Eq. (14)
k	thermal conductivity
$P(t)$	surface averaged direction of descent defined by Eq. (4a)
$P(S_d,t)$	direction of descent defined by Eq. (4b)
$q(S_d,t)$	applied heat flux on drilling surface
$T(\Omega,t)$	estimated temperature
$\Delta T(\Omega,t)$	sensitivity function defined by Eq. (5)
$Y_m(t)$	measured temperature

Greek symbols

β	search step size
$\lambda(\Omega,t)$	Lagrange multiplier defined by Eq. (11)
ϵ	stopping criterion
ρ	density

Superscripts

n	iteration index
$\hat{}$	estimated value

Subscripts

d	drilling surface index
m	sensor index
w	cooling water
∞	ambient condition

iterative inverse algorithm together with the commercial code CFX4.4 [6] has been developed by Huang and Wang [7] who applied the inverse algorithm to estimate the unknown surface heat fluxes in a 3-D solid. By following the similar technique, Huang and Chen [8] estimated the unknown boundary heat flux in a 3-D inverse heat convection problem and Huang and Cheng [9] predicted the heat generation rate of chips on a PC board. Huang et al. [10] developed the technique of Steepest Descent Method (SDM) and commercial code CFX4.4 to estimate the local convective heat transfer coefficients over fin surface in a steady-state 3-D inverse heat conduction problem based on the simulated temperature measurements by infrared thermography. More recently, Huang and Lo [11] applied the similar technique to estimate the applied heat flux on the cutting edges for the cutting tools.

However the 3-D inverse heat conduction problem in estimating the heat flux along the drilling edges for the drilling tool has not been examined. The objective of this study is to extend the techniques used in [7–11] to a transient 3-D inverse drilling problem in estimating the time-dependent heat flux along the drilling edges based on the measured tool temperatures.

The Steepest Descent Method derives basis from the perturbational principle [12] and transforms the inverse problem to the solution of three problems, namely, the direct problem, the sensitivity problem and the adjoint problem, which will be discussed in detail in the next few sections.

2. The direct problem

A practical drilling tool is illustrated in Fig. 1a. The drilling tool is designed to have the coolant holes inside the drill body, $\Omega(x,y,z)$. All the surfaces, except for the top surface and drilling edges, are subjected to a convective

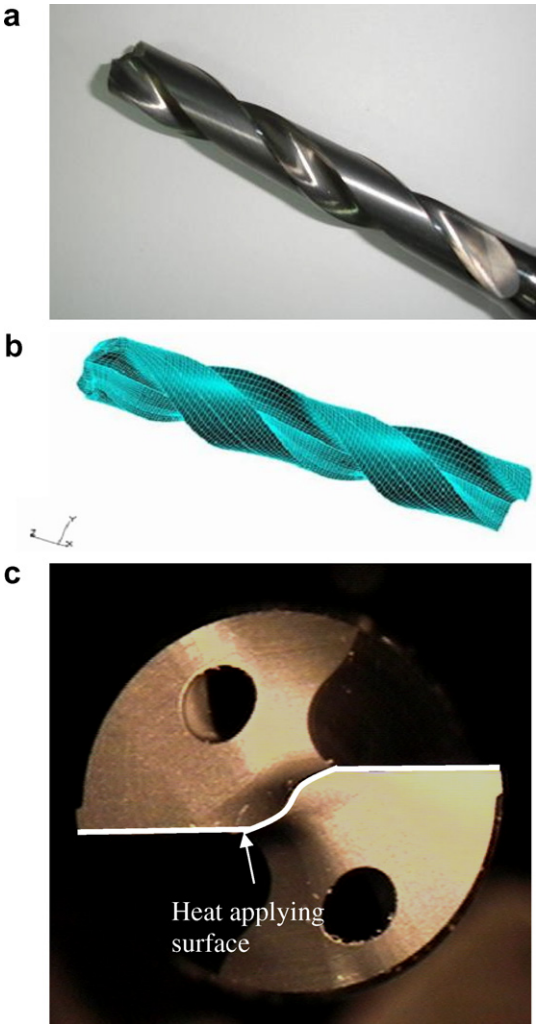

Fig. 1. (a) The drilling tool, (b) the grid system of drilling tool and (c) the heat applying surface.

boundary condition. For the cooling passage surfaces, the prescribed heat transfer coefficient and water temperature are taken as h_w and T_w, respectively. For the surfaces elsewhere, the heat transfer coefficient and ambient temperature are taken as h_∞ and T_∞, respectively. The boundary condition for the top surface is assumed adiabatic and the unknown heat flux is imposed on the drilling surfaces.

The unknown strength of heat flux on the drilling surfaces is assumed only as a function of time. For this reason, an unknown time-dependent heat flux $q(t)$ is imposed on the drilling edges. Fig. 1b shows the simplified grid system (the actual grid system is too dense to be shown) of a drilling tool. Fig. 1c illustrates the heat applying surface along the drilling edges.

The formulation of this 3-D transient drilling problem can be expressed as

$$k\left[\frac{\partial^2 T(\Omega,t)}{\partial x^2}+\frac{\partial^2 T(\Omega,t)}{\partial y^2}+\frac{\partial^2 T(\Omega,t)}{\partial z^2}\right]=\rho C_p\frac{\partial T(\Omega,t)}{\partial t}\quad \text{in } (\Omega,t) \tag{1a}$$

$$-k\frac{\partial T(S_d,t)}{\partial n}=q(t)\quad \text{on the drilling surface } S_d \tag{1b}$$

$$-k\frac{\partial T(S_t,t)}{\partial n}=0\quad \text{on the top surface } S_t \tag{1c}$$

$$-k\frac{\partial T(S_c,t)}{\partial n}=\pm h_w(S_c,t)(T-T_w)\quad \text{on the cooling passage surface } S_c \tag{1d}$$

$$-k\frac{\partial T(S,t)}{\partial n}=\pm h_\infty(S,t)(T-T_\infty)\quad \text{on the surfaces } S \text{ elsewhere} \tag{1e}$$

$$T(\Omega,t)=T_\infty\quad \text{for } t=0 \tag{1f}$$

Here Ω indicates the domain for the drill, k is the thermal conductivity of the material, and ρ and C_p are the density and heat capacity of the material, respectively.

The direct problem considered here is concerned with calculating the drilling tool temperatures when the applied heat flux, heat transfer coefficient, thermal properties as well as the initial and boundary conditions of the drill are all known. The solution for the above 3-D heat conduction problem in the domain $\Omega(x,y,z)$ with time t is solved using CFX4.4 and its Fortran subroutine USRBCS.

3. The inverse problem

For the inverse problem considered here, the time-dependent heat flux $q(t)$ is regarded as being unknown, but everything else in Eq. (1) is known. In addition, the temperature readings using traditional contact type sensors at some proper locations are available.

Let the temperature readings taken by the sensors at the measurement locations be denoted by $Y(x_m,y_m,z_m,t)\equiv Y_m(t)$, here $m=1$ to M and M represents the number of sensors, and (x_m,y_m,z_m) indicates the measurement positions. This inverse problem can be stated as follows: by utilizing the above mentioned measured temperature data $Y_m(t)$, estimate the unknown time-dependent heat flux $q(t)$.

The solution of this inverse problem is to be obtained in such a way that the following functional is minimized:

$$J[q(t)]=\int_{t=0}^{t_f}\sum_{m=1}^{M}[T_m(t)-Y_m(t)]^2\,dt \tag{2}$$

here, $T_m(t)$ are the estimated or computed temperatures at the temperature measurement locations (x_m,y_m,z_m) and time t. These quantities are determined from the solution of the direct problem given previously by using the estimated heat flux $q(t)$.

4. Steepest descent method for minimization

An iterative process based on the following steepest descent method [12] is applied for the estimation of unknown heat flux $q(t)$ by minimizing the functional $J[q(t)]$

$$q^{n+1}(t)=q^n(t)-\beta^n P^n(t)\quad \text{for } n=0,1,2 \tag{3}$$

Here β^n is the search step size from iteration n to iteration $n+1$, and $P^n(t)$ is the surface averaged direction of descent (i.e. search direction) given by

$$P^n(t)=\frac{\int_S\int_{t=0}^{t_f}P^n(S_d,t)\,dt\,dS}{\int_S S_d\,dS} \tag{4a}$$

where

$$P^n(S_d,t)=J'^n(S_d,t) \tag{4b}$$

Eq. (4b) is also the gradient direction at iteration n for steepest descent method.

To complete the iterations in accordance with Eq. (3), the step size and the gradient of the functional $J'^n(S_d,t)$ need be computed. In order to develop expressions in determining these two quantities, a "sensitivity problem" and an "adjoint problem" need be constructed as described below.

4.1. Sensitivity problem and search step size

It is assumed that when $q(t)$ undergoes a variation Δq, T is perturbed by $T+\Delta T$. Then replacing in the direct problem q by $q+\Delta q$ and T by $T+\Delta T$, subtracting the resulting expressions from the direct problem and neglecting the second-order terms, the following sensitivity problem for the sensitivity function ΔT are obtained.

$$k\left[\frac{\partial^2 \Delta T(\Omega,t)}{\partial x^2}+\frac{\partial^2 \Delta T(\Omega,t)}{\partial y^2}+\frac{\partial^2 \Delta T(\Omega,t)}{\partial z^2}\right]=\rho C_p\frac{\partial \Delta T(\Omega,t)}{\partial t}\quad \text{in } (\Omega,t) \tag{5a}$$

$$-k\frac{\partial \Delta T(S_d,t)}{\partial n}=\Delta q(t)\quad \text{on the drilling surface } S_d \tag{5b}$$

$$-k\frac{\partial \Delta T(S_t,t)}{\partial n}=0\quad \text{on the top surface } S_t \tag{5c}$$

$$-k\frac{\partial \Delta T(S_c,t)}{\partial n}=\pm h(S_c,t)\Delta T\quad \text{on the cooling passage surface } S_c \tag{5d}$$

$$-k\frac{\partial \Delta T(S,t)}{\partial n}=\pm h(S,t)\Delta T\quad \text{on the surfaces } S \text{ elsewhere} \tag{5e}$$

$$\Delta T(\Omega,t)=0\quad \text{for } t=0 \tag{5f}$$

CFX 4.4 is used to solve the above sensitivity problem.

The functional $J[q^{n+1}(t)]$ for iteration $n+1$ is obtained by rewriting Eq. (2) as

$$J[q(t)] = \int_{t=0}^{t_f} \sum_{m=1}^{M} [T_m(t; q^n - \beta^n P^n) - Y_m(t)]^2 \, dt \tag{6}$$

where q^{n+1} is replaced by the expression given by Eq. (3). If temperature $T_m(t; q^n - \beta^n P^n)$ is linearized by a Taylor's expansion, Eq. (6) takes the form

$$J[q^{n+1}(t)] = \int_{t=0}^{t_f} \sum_{m=1}^{M} [T_m(t; q^n) - \beta^n \Delta T_m(t; P^n) - Y_m(t)]^2 \, dt \tag{7}$$

where $T_m(t; q^n)$ is the solution of the direct problem at (x_m, y_m, z_m) and t by using the estimate heat flux for the exact heat flux. The sensitivity functions $\Delta T_m(t; P^n)$ are taken as the solutions of problem (5) at the measured positions (x_m, y_m, z_m) and time t by using $\Delta q = P^n$. The search step size β^n is determined by minimizing the functional given by Eq. (7) with respect to β^n. The following expression is the result of β^n:

$$\beta^n = \frac{\int_{t=0}^{t_f} \sum_{m=1}^{M} [T_m(t) - Y_m(t)] \Delta T_m(t) \, dt}{\int_{t=0}^{t_f} \sum_{m=1}^{M} [\Delta T_m(t)]^2 \, dt} \tag{8}$$

4.2. Adjoint problem and gradient equation

To obtain the adjoint problem, Eq. (1a) is multiplied by the Lagrange multiplier (or adjoint function) $\lambda(\Omega, t)$ and the resulting expression is integrated over the correspondent space and time domains. Then the result is added to the right hand side of Eq. (2) to yield the following expression for the functional $J[q(t)]$:

$$\begin{aligned} J[q(t)] = & \int_{t=0}^{t_f} \sum_{m=1}^{M} [T_m(t) - Y_m(t)]^2 \, dt \\ & + \int_{t=0}^{t_f} \int_{\Omega} [\lambda(\Omega, t) \times (\nabla^2 T - \frac{\rho C_p}{k} \frac{\partial T}{\partial t})] d\Omega \, dt \\ = & \int_{t=0}^{t_f} \int_{S} [T(S, t) - Y(S, t)]^2 \delta(x - x_m) \\ & \times \delta(y - y_m) \delta(z - z_m) dS \, dt \\ & + \int_{t=0}^{t_f} \int_{\Omega} [\lambda(\Omega, t) \times (\nabla^2 T - \frac{\rho C_p}{k} \frac{\partial T}{\partial t})] d\Omega \, dt \quad \text{in } (\Omega, t) \end{aligned} \tag{9}$$

where $\delta(\cdot)$ is the Dirac delta function and (x_m, y_m, z_m) refers to the measured positions.

The variation ΔJ can be obtained by perturbing q by $q + \Delta q$ and T by $T + \Delta T$ in Eq. (9), subtracting the resulting expression from the original Eq. (9) and neglecting the second-order terms. We thus find

$$\begin{aligned} \Delta J[q(t)] = & \int_{t=0}^{t_f} \int_{S} 2[T(S, t) - Y(S, t)] \\ & \times \Delta T \delta(x - x_m) \delta(y - y_m) \delta(z - z_m) dS \, dt \\ & + \int_{t=0}^{t_f} \int_{\Omega} [\lambda(\Omega, t) \times (\nabla^2 \Delta T - \frac{\rho C_p}{k} \frac{\partial \Delta T}{\partial t})] d\Omega \, dt \end{aligned} \tag{10}$$

In Eq. (10), the second double integral term is reformulated based on the Green's second identity; the boundary conditions of the sensitivity problem given by Eqs. (5b)–(5e) are utilized and then ΔJ is allowed to go to zero. The vanishing of the integrands containing ΔT leads to the following adjoint problem for the determination of $\lambda(\Omega, t)$:

$$k \left[\frac{\partial^2 \lambda(\Omega, t)}{\partial x^2} + \frac{\partial^2 \lambda(\Omega, t)}{\partial y^2} + \frac{\partial^2 \lambda(\Omega, t)}{\partial z^2} \right] + \rho C_p \frac{\partial \lambda(\Omega, t)}{\partial t} = 0 \quad \text{in } (\Omega, t) \tag{11a}$$

$$-k \frac{\partial \lambda(S_d, t)}{\partial n} = 0 \quad \text{on the drilling surface } S_d \tag{11b}$$

$$-k \frac{\partial \lambda(S_t, t)}{\partial n} = 0 \quad \text{on the top surface } S_t \tag{11c}$$

$$-k \frac{\partial \lambda(S_c, t)}{\partial n} = \pm h(S_c, t) \lambda \quad \text{on the cooling passage surface } S_c \tag{11d}$$

$$\begin{aligned} -k \frac{\partial \lambda(S, t)}{\partial n} = & \pm h(S, t) \lambda + 2k[T(S, t) - Y(S, t)] \\ & \times \delta(x - x_m) \delta(y - y_m) \delta(z - z_m) \\ & \text{on the surfaces } S \text{ elsewhere} \end{aligned} \tag{11e}$$

$$\lambda(\Omega, t_f) = 0 \quad \text{for } t_f = 0 \tag{11f}$$

Finally, the following integral term is left

$$\Delta J = \int_{t=0}^{t_f} \int_{S} -\frac{\lambda(S_d, t)}{k} \Delta q(t) dS \, dt \tag{12}$$

From the definition given in [12], the functional increment can be presented as

$$\Delta J = \int_{t=0}^{t_f} \int_{S} J'(S_d, t) \Delta q(t) dS \, dt \tag{13}$$

A comparison of Eqs. (12) and (13) leads to the following expression for the gradient of the functional $J[q(t)]$:

$$J'(S_d, t) = -\frac{\lambda(S_d, t)}{k} \quad \text{on the drilling surfaces } S_d \tag{14}$$

4.3. Stopping criterion

If the problem contains no measurement errors, the traditional check condition is specified as

$$J[q^{n+1}(t)] < \varepsilon \tag{15}$$

where ε is a small-specified number. However, the observed temperature data may contain measurement errors. Therefore, the functional Eq. (2) is not expected to be equal to

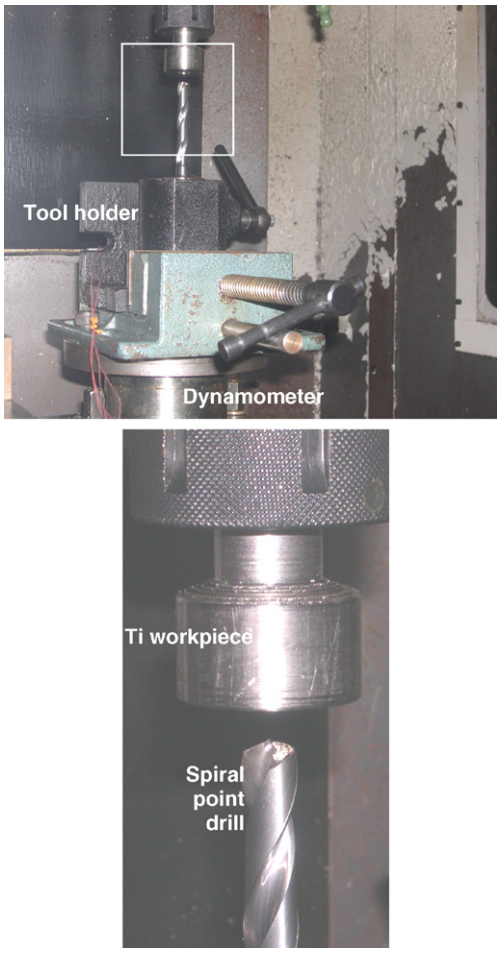

Fig. 2. Experimental setup with workpiece in the spindle and drill in a vertical tool holder.

zero at the final iteration step. As per the experiences of the authors [7–12], the discrepancy principle as the stopping criterion is used in this study, i.e. it is assumed that the temperature residuals may be approximated by

$$T_m(t) - Y_m(t) \approx \sigma, \quad m = 1 \text{ to } M \tag{16}$$

where σ is the standard deviation of the measurements, which is assumed to be a constant. Substituting Eq. (16) into Eq. (2), the following expression is obtained for the stopping criterion ε:

$$\varepsilon = M\sigma^2 t_f \tag{17}$$

The stopping criterion is given by Eq. (15) with ε determined from Eq. (17).

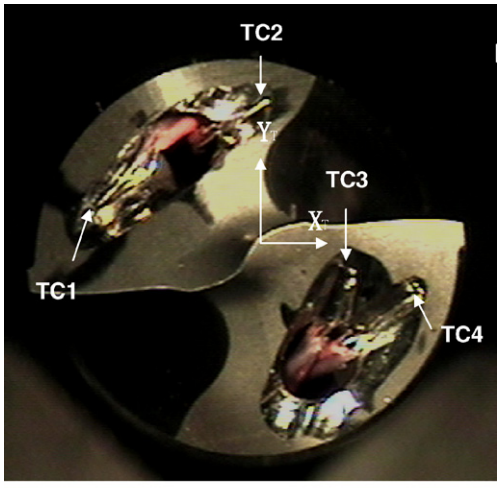

Coordinates of Thermocouples (mm):
TC1 (–3.51, 1.14) TC2 (0.45, 3.60)
TC3 (2.4, –0.51) TC4 (3.93, –0.69)

Fig. 3. The thermocouple locations in the drill flank face.

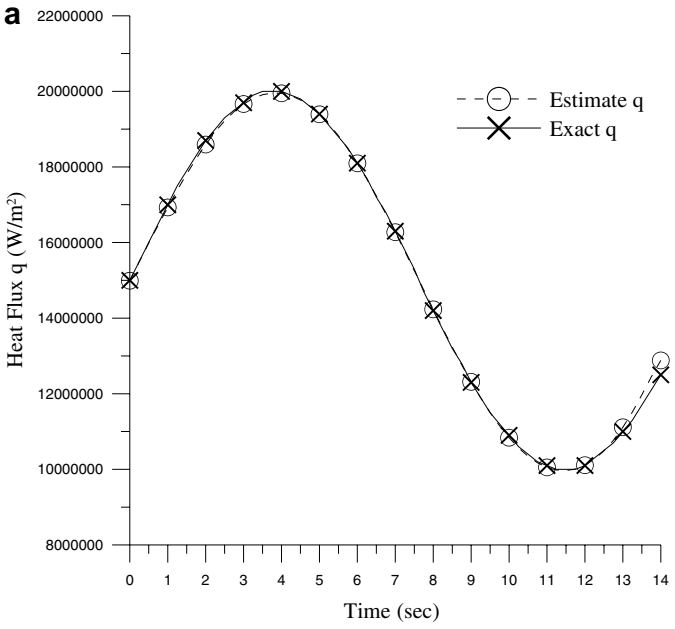

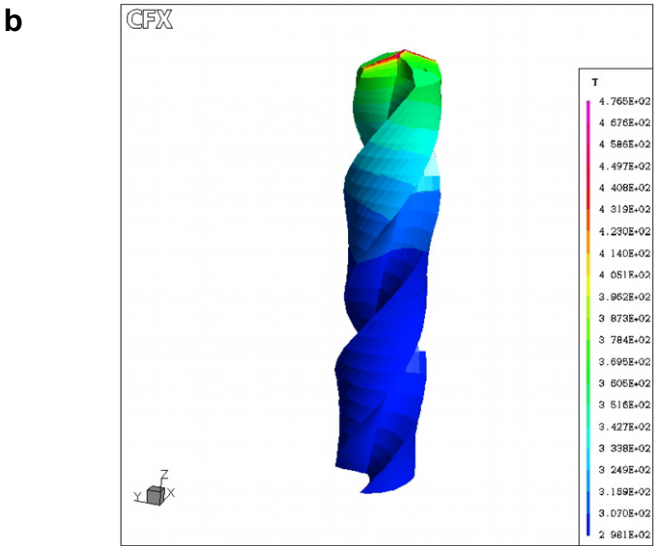

Fig. 4. (a) The exact and estimated heat fluxes and (b) the estimated temperature distributions of the drill at $t = 14$ s, using four sensors and $\sigma = 0$ in the numerical test case.

5. Computational procedure

The computational procedure for the solution of this inverse problem using steepest descent method may be summarized as follows:

Suppose $q^n(t)$ is available at iteration n.

Step 1. Solve the direct problem given by Eq. (1) for $T(\Omega, t)$.
Step 2. Examine the stopping criterion given by Eq. (15) with ε given by Eq. (17). Continue if not satisfied.
Step 3. Solve the adjoint problem given by Eq. (11) for $\lambda(\Omega, t)$.
Step 4. Compute the gradient of the functional J' from Eq. (14).
Step 5. Compute the direction of descent P^n from Eq. (4).
Step 6. Set $\Delta q = P^n$, and solve the sensitivity problem given by Eq. (5) for $\Delta T(\Omega, t)$.
Step 7. Compute the search step size β^n from Eq. (8).
Step 8. Compute the new estimation for q^{n+1} from Eq. (3) and return to Step 1.

6. Experimental setup

The Ti drilling experiment was conducted in a Mori Seiki TV 30 computer numerical control vertical machining center. Fig. 2 shows the experimental setup with the stationary drill and the Ti workpiece driven by spindle. The drill was stationary because four thermocouples embedded on the flank face could be routed through coolant holes in the drill body to a data acquisition system during drilling [13]. The drill and machine spindle axes were aligned by a test indicator installed in the spindle. The location of drill was adjusted in the horizontal plane until the eccentricity was less than 10 μm. The tilt

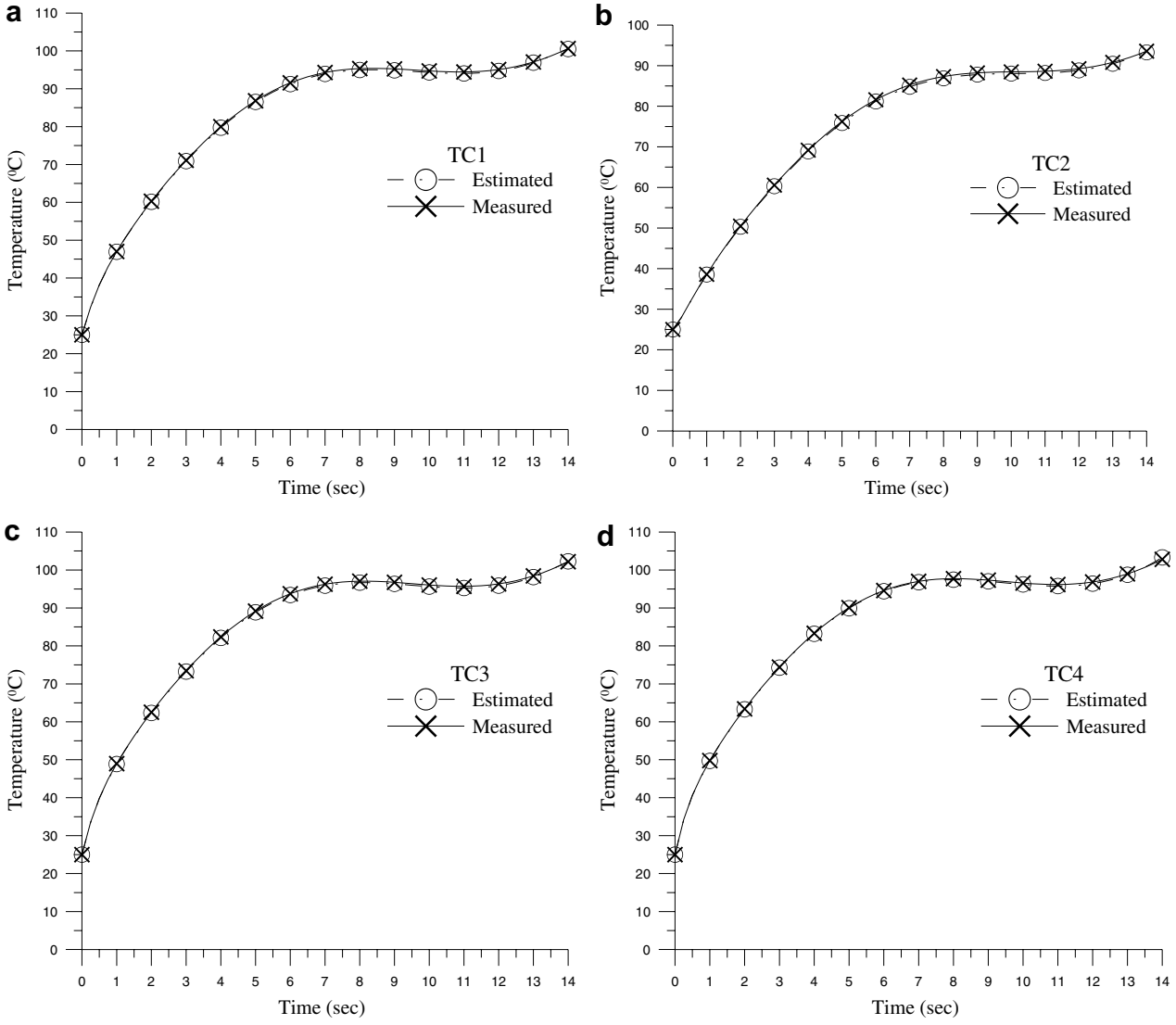

Fig. 5. The measured and estimated temperature distributions of the drill at (a) TC1, (b) TC2, (c) TC3 and (d) TC4 in the numerical test case.

of the drill was adjusted so that two planes, which were 5 cm apart in height, still both had less than 10 μm eccentricity. A Kistler 9272 dynamometer was placed under the drill holder to measure the thrust force and torque.

The workpiece was a 38 mm diameter grade two commercially pure (CP) Ti bar. The drill was a 9.92 mm diameter spiral point drill, Kennametal K285A03906, with S-shaped chisel edge. Compared to a conventional twist drill, the chisel edge had lower negative rake angle. Therefore, the web could participate in cutting, not just indenting the workpiece like the conventional twist drill. The spiral point drill geometry can reduce the thrust force and make the drill self-centering [14].

Fig. 3 shows the spiral point drill and locations of four thermocouples on the drill frank surface. An $X_T Y_T$ coordinate with the X_T-axis parallel to the tangential of the apex of the curved cutting edge is defined. The tip of 0.127 mm diameter type E thermocouples (OMEGA 5TC-TT-E-36-72) was installed at the edge of hand-ground slots on the drill flank face. Four thermocouples are denoted as TC1, TC2, TC3 and TC4, and arranged at different locations on the flank surface, as shown in Fig. 3. The $X_T Y_T$ coordinate of four thermocouples are given as (−3.51 mm,

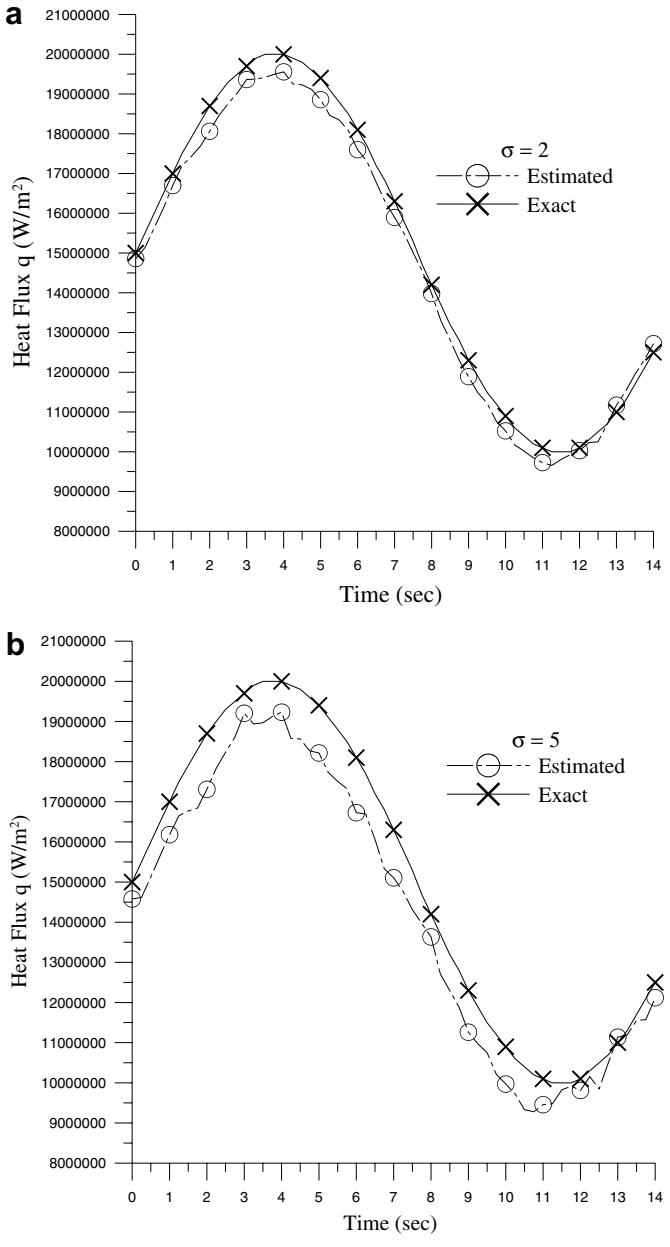

Fig. 6. The exact and estimated heat fluxes with (a) $\sigma = 2$ °C and (b) $\sigma = 5$ °C in the numerical test case.

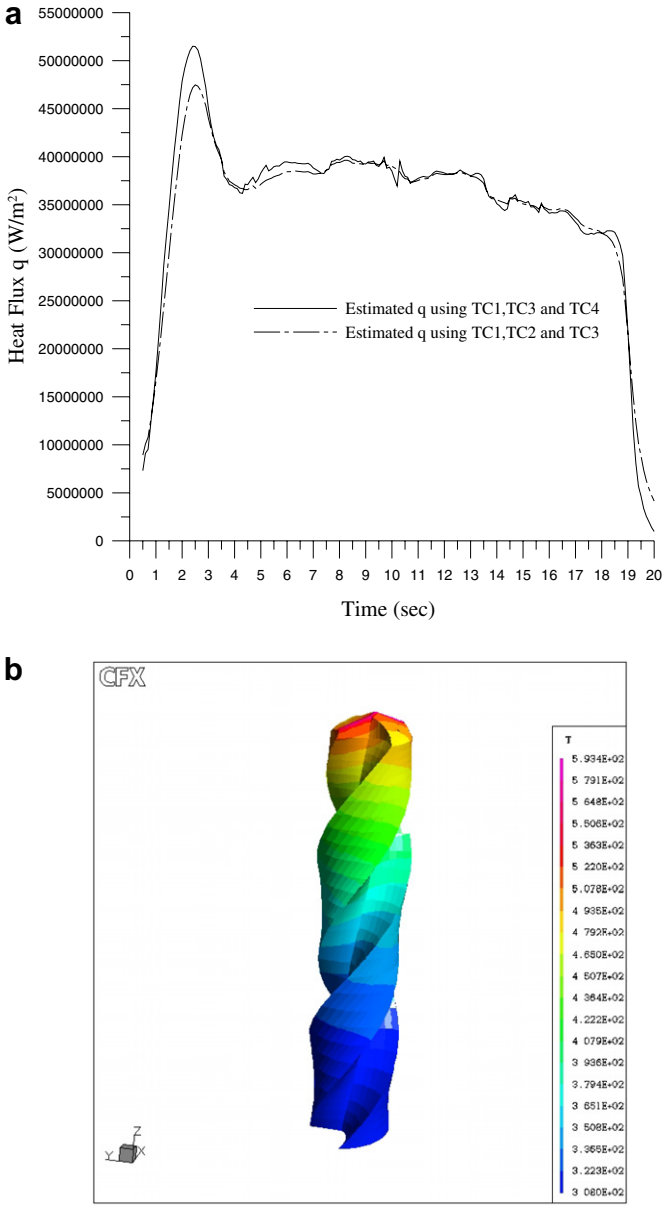

Fig. 7. (a) The estimated applied heat fluxes using (1) TC1, TC2 and TC3, and (2) TC1, TC3 and TC4 measurements, respectively; and (b) the estimated temperature distributions of the drill at $t = 19.2$ s and 780 rpm drilling speed.

1.14 mm), (0.45 mm, 3.60 mm), (2.4 mm, −0.51 mm) and (3.93 mm, −0.69 mm), respectively, and is also listed in Fig. 3.

TC1 is located close to the cutting edge and away from the drill center. TC2 is placed close to the flute and away from the drill center. TC3 and TC4 are both near the cutting edge with TC3 close to and TC4 away from the drill center. Thermocouples were covered with cement (Omega OB-400) to secure the position and prevent the contact with workpiece.

Two drilling tests were conducted at two spindle speeds, 780 and 2350 rpm, which correspond to 24.4 and 73.2 m/min drill peripheral cutting speeds, respectively. The feed was fixed at 0.051 mm/rev or 0.025 mm for each tooth of the two-flute drill. All experiments were conducted dry without cutting fluid.

7. Results and discussion

The objective of this study is to show the validity of the SDM in predicting the unknown time-dependent heat flux along the drilling edges for a 3-D drilling tool with no prior information on the functional form of the unknown quantities. The physical model for this problem is described as follows: All experiments were conducted dry without cutting fluid, therefore $h_\infty = h_w = 30\ \mathrm{W/(m^2\ K)}$.

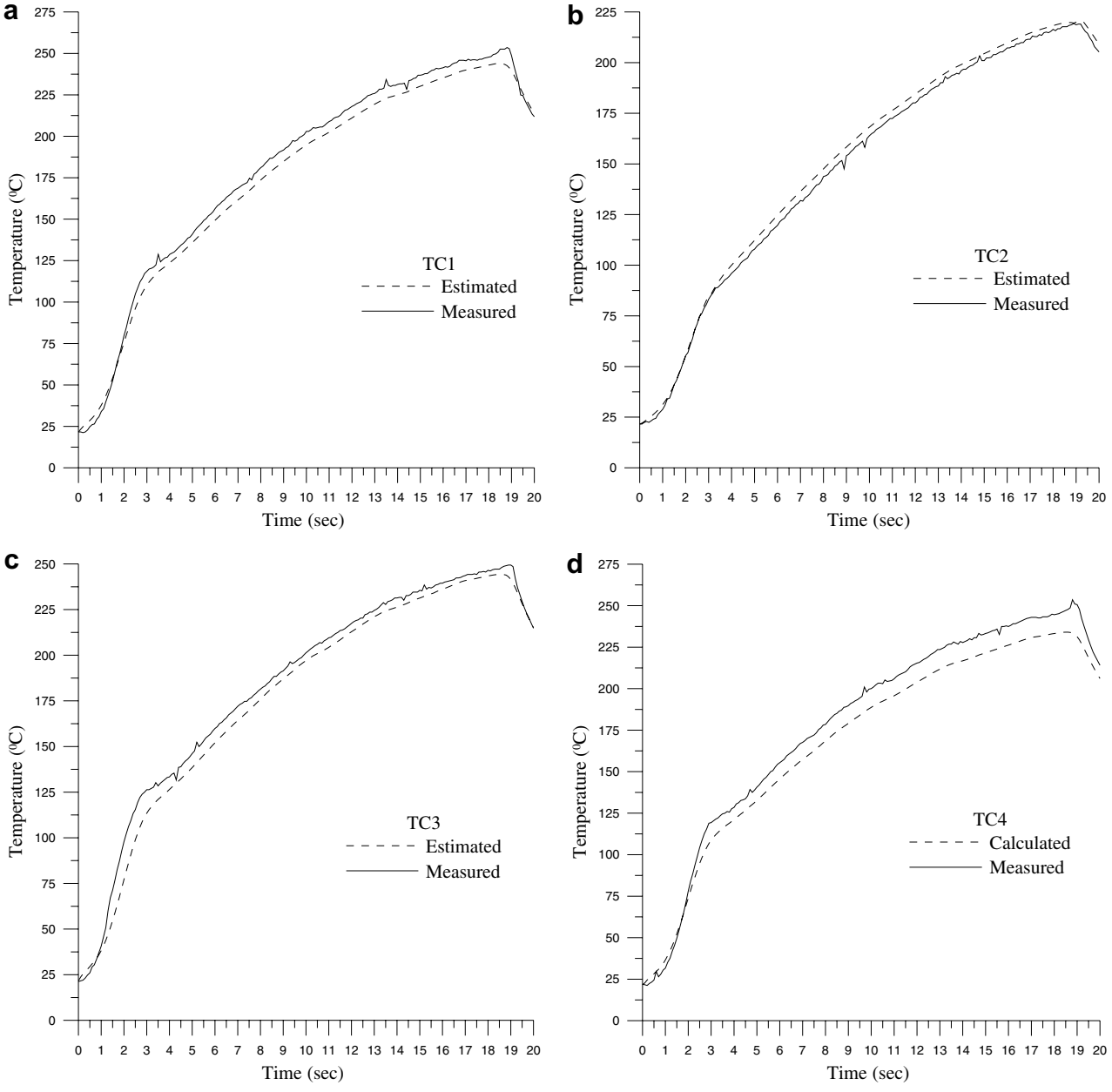

Fig. 8. The measured and estimated temperatures at (a) TC1, (b) TC2 and (c) TC3 at 780 rpm drilling speed, and (d) the measured and calculated temperatures (using estimated heat flux) at TC4.

7.1. Numerical experiments

To illustrate the ability of the SDM in predicting $q(t)$ with inverse analysis from the knowledge of the simulated measured temperature distributions at the measured positions (x_m, y_m, z_m), we consider the following numerical test cases.

One of the advantages of using the SDM is that the initial guesses of the unknown heat fluxes $q(t)$ can be chosen arbitrarily. In all the test cases considered here, the initial guesses for heat fluxes are taken as $q(t) = 0.0$.

In order to compare the results for situations involving random measurement errors, we assume normally distributed uncorrelated errors with zero mean and constant standard deviation. The simulated inexact measurement data Y_m can be expressed as

$$Y_m = Y_{m,\text{exact}} + \omega\sigma \tag{18}$$

where $Y_{m,\text{exact}}$ is the solution of the direct problem with the exact heat flux; σ is the standard deviation of the measurements; and ω is a random variable that generated by subroutine DRNNOR of the IMSL [15], ω is within -2.576 to 2.576 for a 99% confidence bound.

The geometry and grid system of the drilling tool for the numerical test case are shown in Fig. 1. The number of grid in Ω is taken as 9424. The total grid number on S_d plane is

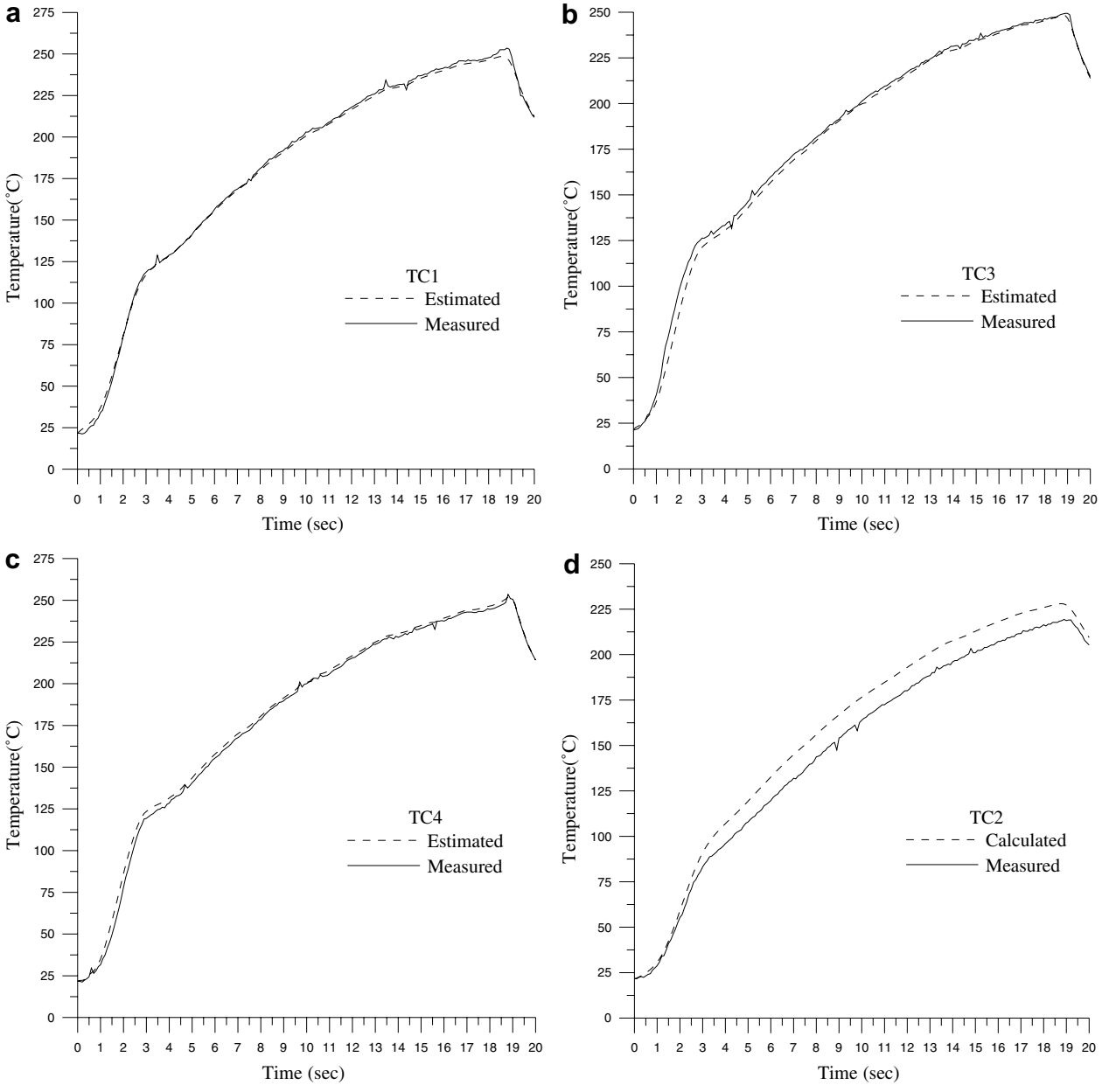

Fig. 9. The measured and estimated temperatures at (a) TC1, (b) TC3 and (c) TC4 at 780 rpm drilling speed, and (d) the measured and calculated temperatures (using estimated heat flux) at TC2.

46. The temperature measurement locations are at the grid points. The measurement time period Δt is 0.25 s and the total measurement time t_f is 15 s, i.e. there are 56 time steps. Besides $T_\infty = T_w = 25\ ^\circ C$ are used.

The simulated exact function of the surface heat fluxes on drilling surface S_d in this numerical experiment is given as

$$q(S_d, t) = 15000000 + 5000000 \times \sin\left[\frac{2\pi t}{15}\right] \text{W/m}^2 \quad \text{on } S_{ci}, \quad 0 \leqslant t \leqslant 15 \text{ s} \tag{19}$$

A three-dimensional inverse problem is firstly examined by using exact measurements, i.e. $\sigma = 0.0$. By setting stopping criteria $\varepsilon = 7.5$, after 30 iterations the inverse solutions converged. Due to the singularity of the gradient at final time, the estimated values at last few time intervals are discarded and therefore the average estimated heat flux is shown just up to $t = 14$ s. The exact and the estimated heat fluxes and the estimated drill temperature distributions at $t = 14$ s are shown in Fig. 4a and b, respectively.

The estimated heat flux is close to the exact values. The relative error between exact and estimated heat flux is calculated as ERRq = 2.32%, where ERRq is defined as

$$\text{ERRq}\% = \left[\sum_{t=1}^{14}\left|\frac{q(t) - \hat{q}(t)}{q(t)}\right|\right] \Big/ 14 \times 100\% \tag{20}$$

here t represents the index of discreted time and $\hat{q}(t)$ indicates the estimated heat flux.

The measured and estimated temperature distributions of the drill at TC1, TC2, TC3 and TC4 are shown in Fig. 5. It can be seen that they are all in a good agreement since the relative errors between them are calculated as $\text{ERRT}_1 = 0.0746\%$, $\text{ERRT}_2 = 0.0929\%$, $\text{ERRT}_3 = 0.0827\%$ and $\text{ERRT}_4 = 0.0624\%$, respectively, where ERRT_m is defined as

$$\text{ERRT}_m\% = \left[\sum_{t=1}^{14}\left|\frac{T_m(t) - Y_m(t)}{Y_m(t)}\right|\right] \Big/ 14 \times 100\%, \quad m = 1 \text{ to } 4 \tag{21}$$

here t represents the index of discreted time.

The inverse calculation is then proceeded to consider the situation of inexact temperature measurements. The standard deviation of the measurement error is first taken as $\sigma = 2\ ^\circ C$, then it is increased to $\sigma = 5\ ^\circ C$.

For $\sigma = 2\ ^\circ C$, 20 iterations are needed to satisfy the stopping criterion based on the discrepancy principle, the exact and estimated heat fluxes are shown in Fig. 6a. The relative errors for the heat fluxes and temperatures are calculated as ERRq = 3.39%, $\text{ERRT}_1 = 0.51\%$, $\text{ERRT}_2 = 0.514\%$, $\text{ERRT}_3 = 0.436\%$ and $\text{ERRT}_4 = 0.431\%$, respectively. For $\sigma = 5\ ^\circ C$, the number of iterations to satisfy the stopping criterion is only 14, the exact and estimated heat fluxes are shown in Fig. 6b, and the relative errors for heat flux and temperatures are calculated as ERRq = 6.28%, $\text{ERRT}_1 = 1.08\%$, $\text{ERRT}_2 = 0.982\%$, $\text{ERRT}_3 = 1.07\%$ and $\text{ERRT}_4 = 1.07\%$, respectively.

It can be learned based on the above numerical results that the estimated heat fluxes are still reliable when using four sensor measurements and considering error measurements.

7.2. Experimental analysis

In order to show the practical applications for the present inverse algorithm to the inverse drilling problem in estimating the applied heat flux for a drill, the measured temperature at four sensors as stated in Section 5 are uti-

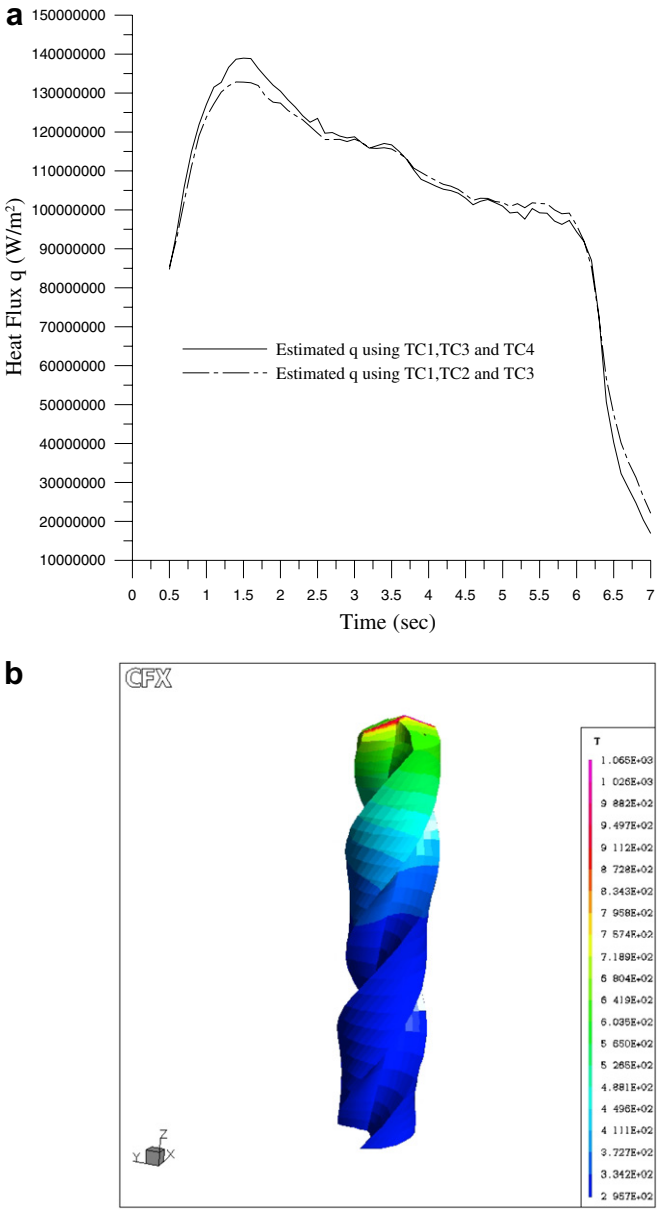

Fig. 10. (a) The estimated applied heat fluxes using (1) TC1, TC2 and TC3, and (2) TC1, TC3 and TC4 measurements, respectively; and (b) the estimated temperature distributions of the drill at $t = 6.4$ s and 2350 rpm drilling speed.

lized. Two cases are considered here: (1) temperatures obtained at TC1, TC2 and TC3 are used as the measured temperatures, while the temperatures measured at TC4 is used as the purpose of verification; (2) temperatures obtained at TC1, TC3 and TC4 are used as the measured temperatures, while the temperatures measured at TC2 is used as the checking temperature. Finally, the inverse solutions obtained by the above two cases will be compared.

The ambient and water temperatures, T_∞ and T_w, are taken as the initial measured temperature of the drill at TC1 for all the inverse calculations considered in the section of experimental analysis. First, the estimated heat flux q at the spindle speed 780 rpm, which correspond to 24.4 m/min drill peripheral cutting speed, based on the temperature measurements at (TC1, TC2, TC3) and (TC1, TC3, TC4), respectively, are shown in Fig. 7a. The estimated drill temperature distributions at $t = 19.2$ s is reported in Fig. 7b. It can be learned from Fig. 7b that the drilling edges always have the highest temperatures.

The measured and estimated temperatures at TC1, TC2 and TC3 are illustrated in Fig. 8a, b and c, respectively. It can be seen from these three figures that they are in a good agreement. The relative errors at TC1, TC2 and TC3 are calculated as $\mathrm{ERRT}_1 = 4.15\%$, $\mathrm{ERRT}_2 = 2.55\%$ and $\mathrm{ERRT}_3 = 4.52\%$, respectively.

In order to verify the accuracy of the present inverse algorithm, the temperature at TC4 is calculated by using the estimated heat flux. The comparison of the measured

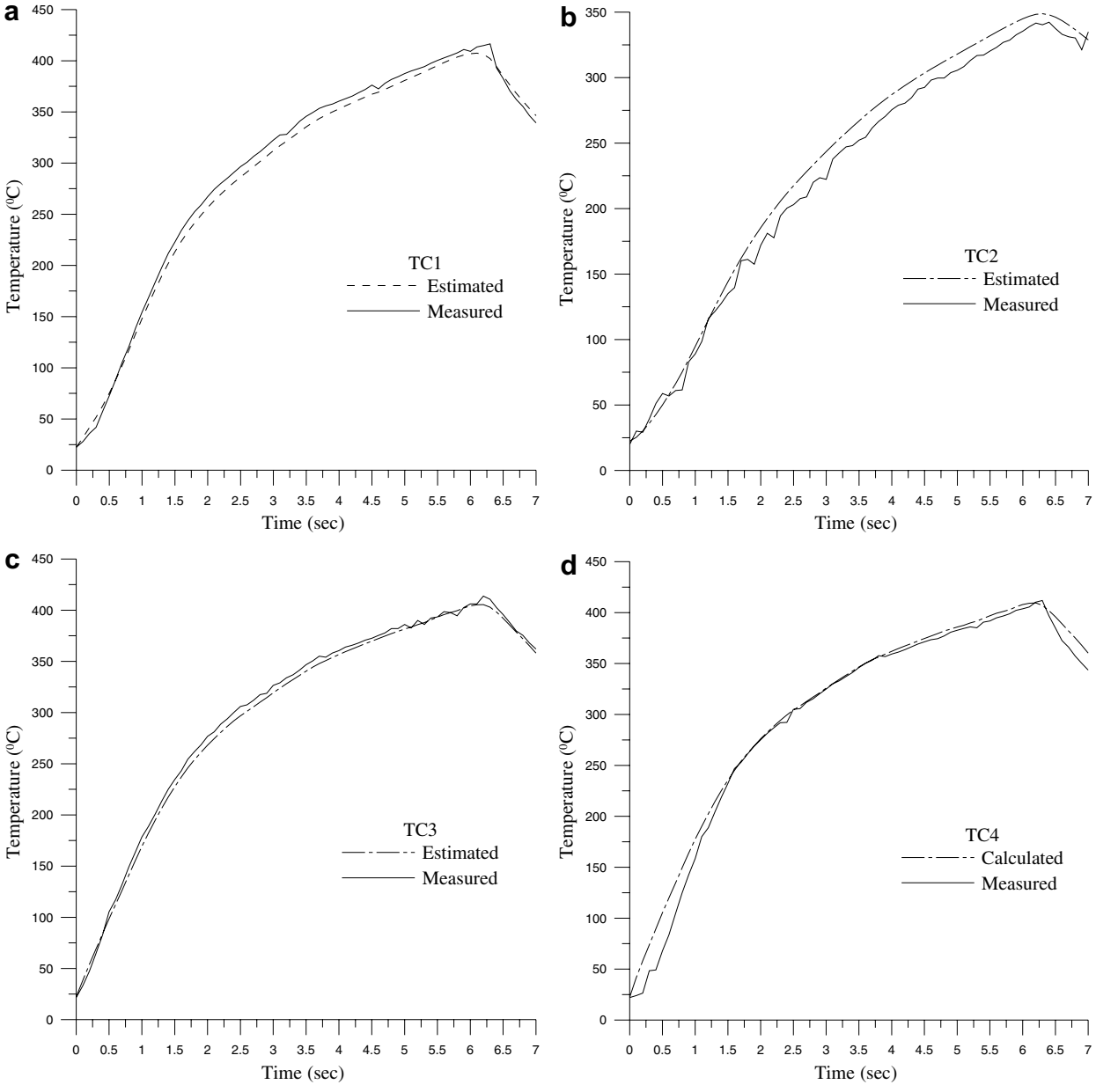

Fig. 11. The measured and estimated temperatures at (a) TC1, (b) TC2 and (c) TC3 at 2350 rpm drilling speed, and (d) the measured and calculated temperatures (using estimated heat flux) at TC4.

and calculated temperatures at TC4 is plotted in Fig. 8d. The relative error is calculated as $ERRT_4 = 6.0344\%$.

The measured and estimated temperatures at TC1, TC3 and TC4 are illustrated in Fig. 9a, b and c, respectively. The comparison of the measured and calculated temperatures at TC2 is plotted in Fig. 9d. The relative errors at TC1, TC3, TC4 and TC2 are calculated as $ERRT_1 = 1.453\%$, $ERRT_3 = 2.215\%$, $ERRT_4 = 2.078\%$ and $ERRT_2 = 7.192\%$, respectively. This implies that the present estimated heat flux is indeed the actual drilling heat flux since the residual between the checking and measuring temperatures are always within the reliable range.

The estimated heat flux is increased in the beginning of drilling, this may be due to the fact that the applied torque is also increased in the beginning of drilling. The heat flux is then decreased till the penetration of the titanium plate. The total area of heat applying surface is calculated from Fig. 1c as about $1.275 \times 10^{-7}\,m^2$, the total applied heat flux can be readily obtained by multiplying the estimated q with that area.

Next, the estimated heat flux q at the spindle speed 2350 rpm, which correspond to 73.2 m/min drill peripheral cutting speed, based on the temperature measurements at (TC1, TC2, TC3) and (TC1, TC3, TC4) are shown in

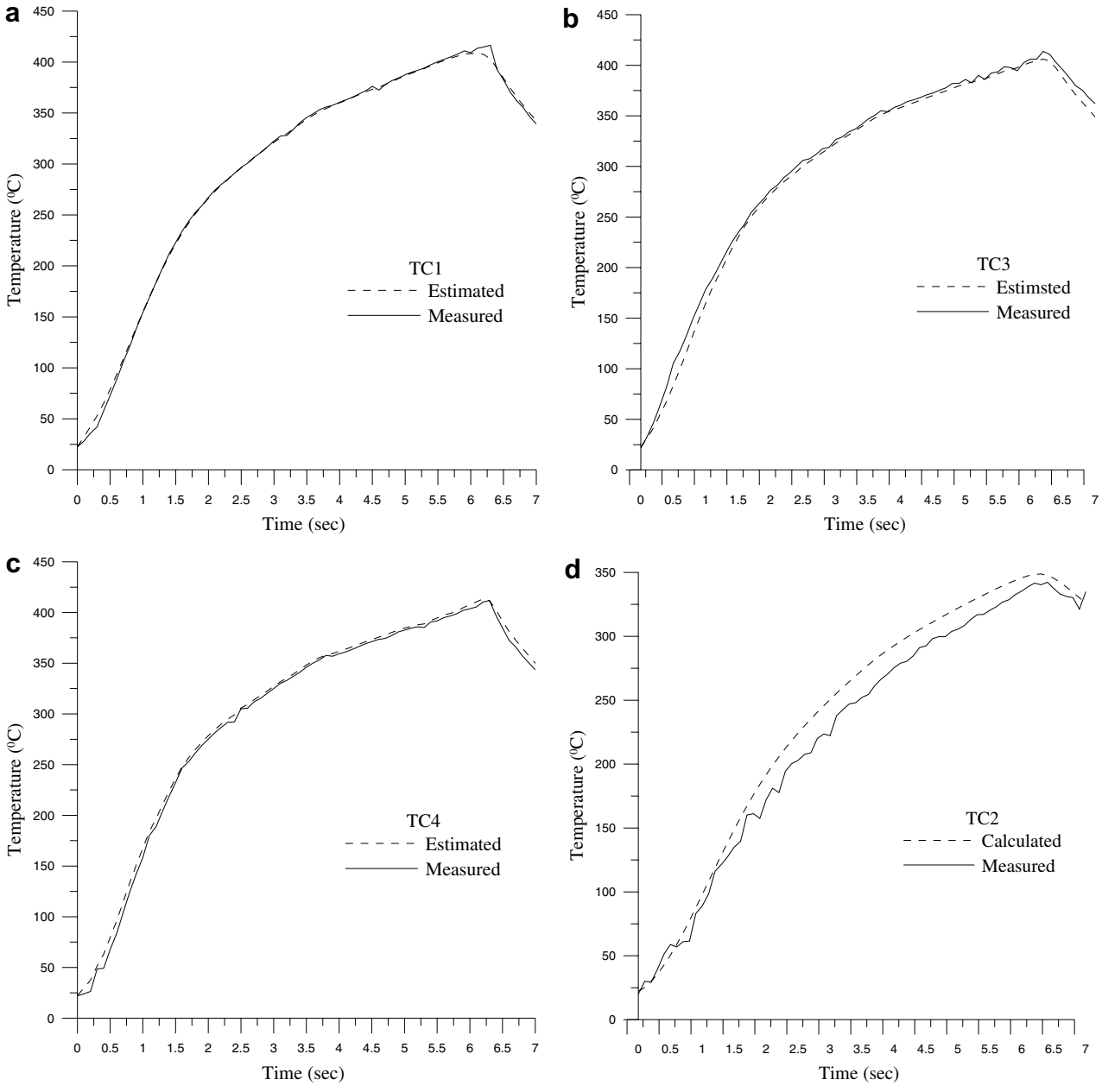

Fig. 12. The measured and estimated temperatures at (a) TC1, (b) TC3 and (c) TC4 at 2350 rpm drilling speed, and (d) the measured and calculated temperatures (using estimated heat flux) at TC2.

Fig. 10a. The estimated drill temperature distributions at $t = 6.4$ s is reported in Fig. 10b. Again, the highest drilling temperature occurs along the drilling edges. The measured and estimated temperatures at TC1, TC2 and TC3 are illustrated in Fig. 11a, b and c, respectively. The relative errors at TC1, TC2 and TC3 are calculated as $ERRT_1 = 3.22\%$, $ERRT_2 = 5.57\%$ and $ERRT_3 = 2.33\%$, respectively.

The temperature at TC4 is calculated for the purpose of verification by using the estimated heat flux. The comparison of the measured and calculated temperatures at TC4 is plotted in Fig. 11d. The relative error is calculated as $ERRT_4 = 5.29\%$.

The measured and estimated temperatures at TC1, TC3 and TC4 are illustrated in Fig. 12a, b and c, respectively. The comparison of the measured and calculated temperatures at TC2 is plotted in Fig. 12d. The relative errors at TC1, TC3, TC4 and TC2 are calculated as $ERRT_1 = 1.68\%$, $ERRT_3 = 2.90\%$, $ERRT_4 = 3.21\%$ and $ERRT_2 = 7.39\%$, respectively.

Again, due to the increasing of the applied torque, the estimated heat flux is increased in the beginning of drilling. Thereafter the heat flux is decreased till the penetration of the working piece. The applied total can be obtained by multiplying the estimated q with the heat applying area $1.275 \times 10^{-7}\,m^2$.

It may be of interest to compare the applied heat flux with time for low and high speed drilling. The rate of increasing of the applied heat flux at low drilling speed is very steep, after that the rate of decreasing of the applied heat flux is also very steep, finally it decreases slowly until the penetration of the plate. However, the rate of increasing of the applied heat flux at high drilling speed is not that steep like low drilling speed and the rate of decreasing of the applied heat flux remains stable. This may be concluded that the drilling thermal condition for high speed drilling is better than that for low speed drilling since more stable applied heat flux is experienced.

Finally it can be concluded from the above numerical test cases and experimental analysis that the SDM is now applied successfully in this 3-D inverse drilling problem for predicting the time-dependent surface heat fluxes of the drilling tools.

8. Conclusions

The SDM with adjoint equation was successfully applied in a 3-D inverse heat conduction problem in determining the time-dependent applied heat flux of a tool in the titanium drillings. The numerical test cases involving different measurement errors were considered. The results show that the SDM does not require a priori information for the functional form of the unknown functions and the reliable estimated values can always be obtained. Finally, the experimental data are utilized to estimate the actual applied heat flux on the drilling edge for the drilling tool. It is found that in the beginning the applied heat flux is increased with time due to the increasing of the torque, then the applied heat flux is decreased till the penetration of the workpiece.

Acknowledgment

This work was supported in part through the National Science Council, ROC, Grant No. NSC-94-2611-E-006-003.

References

[1] K. Sakurai, K. Adachi, K. Ogawa, R. Niba, Drilling of Ti–6Al–4V alloy, Keikinzoku/J. Jpn. Inst. Light Met. 42 (1992) 389–394.
[2] K. Sakurai, K. Adachi, K. Ogawa, Low frequency vibratory drilling of Ti–6Al–4V alloy, Keikinzoku/J. Jpn. Inst. Light Met. 42 (1992) 633–637.
[3] K. Sakurai, K. Adachi, T. Kamekawa, K. Ogawa, S. Hanasaki, Intermittently decelerated feed drilling of Ti–6%Al–4%V alloy, Keikinzoku/J. Jpn. Inst. Light Met. 46 (1996) 138–143.
[4] M. Arai, M. Ogawa, Effects of high pressure supply of cutting fluid in drilling of titanium alloy, Keikinzoku/J. Jpn. Inst. Light Met. 47 (1997) 139–144.
[5] J. Cantero, M. Tardío, J. Canteli, M. Marcos, M. Miguélez, Dry drilling of alloy Ti–6Al–4V, Int. J. Mach. Tool. Manuf. 45 (2005) 1246–1255.
[6] CFX-4.4 User's Manual, AEA Technology Plc, Oxfordshire, UK, 2001.
[7] C.H. Huang, S.P. Wang, A three-dimensional inverse heat conduction problem in estimating surface heat flux by conjugate gradient method, Int. J. Heat Mass Transfer 42 (1999) 3387–3403.
[8] C.H. Huang, W.C. Chen, A three-dimensional inverse forced convection problem in estimating surface heat flux by conjugate gradient method, Int. J. Heat Mass Transfer 43 (2000) 3171–3181.
[9] C.H. Huang, S.C. Cheng, A three-dimensional inverse problem of estimating the volumetric heat generation for a composite material, Numer. Heat Transfer, Part A 39 (2001) 383–403.
[10] C.H. Huang, I.C. Yuan, H.A. Ay, Three-dimensional inverse problem in imaging the local heat transfer coefficients for plate finned-tube heat exchangers, Int. J. Heat Mass Transfer 46 (2003) 3629–3638.
[11] C.H. Huang, H.C. Lo, A three-dimensional inverse problem in predicting the heat fluxes distribution in the cutting tools, Numer. Heat Transfer, Part A—Appl. 48 (2005) 1009–1034.
[12] O.M. Alifanov, Inverse Heat Transfer Problem, Springer-Verlag, Berlin, 1994.
[13] J.S. Agapiou, D.A. Stephenson, Analytical and experimental studies of drill temperatures, J. Eng. Ind. 116 (1994) 54–60.
[14] H. Ernst, W.A. Haggerty, Spiral point drill – new concept in drill point geometry, ASME Trans. 80 (1958) 1059–1072.
[15] IMSL Library Edition 10.0. User's Manual: Math Library Version 1.0, IMSL, Houston, TX, 1987.